Journal of Quantitative Spectroscopy & Radiative Transfer 112 (2011) 632–645

Contents lists available at ScienceDirect

Journal of Quantitative Spectroscopy & Radiative Transfer

journal homepage: www.elsevier.com/locate/jqsrt

Radiation propagation in random media: From positive to negative correlations in high-frequency fluctuations

Anthony B. Davis [a,*], Mark B. Mineev-Weinstein [b,1]

[a] Jet Propulsion Laboratory, California Institute of Technology, Pasadena, CA 91109, USA
[b] Los Alamos National Laboratory, Solid Mechanics and Material Properties (X-1-SMMP), Los Alamos, NM 87545, USA

ARTICLE INFO

Keywords:
Multi-dimensional radiation transport
Stochastic media
Non-exponential transmission laws
Clustering/anti-clustering material particles
Negative spatial correlations

ABSTRACT

We survey research on radiation propagation or ballistic particle motion through media with randomly variable material density, and we investigate the topic with an emphasis on very high spatial frequencies. Our new results are based on a specific variability model consisting of a zero-mean Gaussian scaling noise riding on a constant value that is large enough with respect to the amplitude of the noise to yield overwhelmingly non-negative density. We first generalize known results about sub-exponential transmission from regular functions, which are almost everywhere continuous, to merely "measurable" ones, which are almost everywhere discontinuous (akin to statistically stationary noises), with positively correlated fluctuations. We then use the generalized measure-theoretic formulation to address negatively correlated stochastic media without leaving the framework of conventional (continuum-limit) transport theory. We thus resolve a controversy about recent claims that only discrete-point process approaches can accommodate negative correlations, i.e., anti-clustering of the material particles. We obtain in this case the predicted super-exponential behavior, but it is rather weak. Physically, and much like the alternative discrete-point process approach, the new model applies most naturally to scales commensurate with the inter-particle distance in the material, i.e., when the notion of particle density breaks down due to Poissonian—or maybe not-so-Poissonian—number-count fluctuations occur in the sample volume. At the same time, the noisy structure must prevail up to scales commensurate with the mean-free-path to be of practical significance. Possible applications are discussed.

© 2010 Elsevier Ltd. All rights reserved.

1. Introduction, context, and overview

Although radiative transfer theory is highly developed for uniform or slowly varying optical media, natural optical media are often variable at all observable scales. Clouds are a good example where in situ probing by aircraft show highly variable extinction as well as liquid water content. Being highly turbulent dynamical environments, the fluctuations of an admixture such as condensed water particles in clouds ($\sim$ 10 s of μm in size) are expected over a huge range of scales: down to the Kolmogorov dissipation scale ($\sim$ a few mm) and up to the cloud-system scale ($\sim$ 10 s of km). Somewhere in this range are the radiatively relevant scales such as the mean-free-path, or e-folding distance, for solar (thermal) radiation propagation between (emission,) scattering, absorption, or escape events in the transport process. As contrived as they are, nuclear engineering systems (e.g., reactors) can also exhibit macroscopic cross-section variations over a very wide range of scales. So wide as to challenge the memory requirements and the related efficiency of the most detailed computational transport models.

There is an obvious qualitative difference between these two examples. A priori, cloud structure is inherently random except maybe at the largest scales where, for instance, clouds often exhibit strong gradients in the vertical. By contrast, we

* Corresponding author. Tel.: +1 818 354 0450; fax: +1 818 393 4619.
E-mail address: Anthony.B.Davis@jpl.nasa.gov (A.B. Davis).
[1] Now at: Max Planck Institute for the Physics of Complex Systems, Nöthnitzer Straße 38, 01187 Dresden, Germany.

0022-4073/$ - see front matter © 2010 Elsevier Ltd. All rights reserved.
doi:10.1016/j.jqsrt.2010.10.001

envision nuclear systems as carefully designed down to the smallest detail. And then there are pebble-bed reactors, a relatively new concept, where small ($\sim$6 cm diameter) spherical pellets are stacked randomly in a large vessel; these pellets are themselves made of a graphite shell filled with tiny ($\sim$1 mm diameter) spheres of fuel surrounded by other materials.[2] Here again, the scales of variability straddle the neutron mean-free-paths of the various materials, including the fluid between the pellets.

In short, transport media whose material properties can only be described in practice by statistical methods are playing increasingly important roles in atmospheric radiative transfer (e.g., the role of clouds in the large-scale radiative energy budget), in nuclear engineering (e.g., above-mentioned next-generation reactors or fractures in shielding materials), in medical physics (e.g., dosimetry and computed tomography), in astrophysics (e.g., convectively unstable stars), and so on. If the 3D spatial structure of the optical medium can only be described in probabilistic terms, then one can only ask of the corresponding transport theory to deliver domain-average quantities. Two broad classes of solutions have emerged for such transport problems: "homogenization" and, broadly speaking, "alternate transport theories." In the former pursuit, one seeks ways of redefining the material properties of the medium, as if it were uniform at the (usually large) scales of interest, but in a manner that accounts for the dominant effects of smaller scale (usually unresolved) variability. In the later approach, one arrives at new transport equations, to be solved analytically or numerically.

Homogenization (a.k.a. the "effective medium" approach) is very attractive because it reduces the difficult multi-dimensional problem to a much simpler problem for a uniform medium, which has known solutions (at least in 1D, using slab geometry). For examples in the atmospheric literature, see Davis et al. [1], Cahalan et al. [2,3], Cairns et al. [4], and Petty [5]. For examples from nuclear engineering, see Graziani [6] and Olsen et al. [7,8].

Although they pose new technical challenges, new transport equations describing the stochastic transport problem are generally a more realistic approach. A well-known example is the theory of transport in Markovian binary mixtures, which is expressed as a pair of coupled integro-differential transport equations; it has been surveyed in great depth by Pomraning [9], Byrne [10], and Kassianov and Lane [11, in this Special Issue], respectively, from the particle transport, radiative transfer (RT), and broader perspectives. There are other such mean-field transport theories, for instance, Stephens [12] reconsiders the classic two-stream model in 1D RT in a manner that incorporates some 3D RT phenomenology uncovered in his numerical simulations [13]. As another example, Davis and Marshak [14–16] have developed diffusion and transport theories, where the particle free-path distributions have power-law tails to represent the mean propagation kernel for heterogeneous media.

Between homogenization theories and alternative transport equations, there is an intermediate approach to transport in stochastic media, very popular in the atmospheric community, is the independent pixel (or column) approximation—the IPA (or ICA). Therein, one solves the 1D RT problem for given optical properties, but one or more of these parameters are actually random variables with given probability density functions (PDFs). Typically, the optical depth of the medium is varied. In the IP(C)A, one simply averages the outcome of the 1D RT computation weighted by the known PDF. Although the concept goes at least as far back as the 1972 report by Mullamaa et al. [17], the terminology was introduced in the mid-1990's [18,19]. The IP(C)A was used originally to derive closed-form expressions, including one or more new parameters for the variability, but more recently it has been implemented numerically, particularly with global climate models in mind [20–22].

There is an interesting and important question about transport in random optical media that is more elementary than all of the above solutions, which is simply to characterize propagation between emission, scattering, absorption, and detection/escape events. Studies are on-going, for instance, in chord-length distributions[3] for media made of closely packed disks or spheres [7,8]. We see this question as one about the prevailing law of direct transmission, which is closely related to the PDF for the free paths covered by the transported particles. Imagining a (pulsed) point source, how many particles are stopped near (early) versus far (late)? The standard answer is: an exponential distribution, the famous Bouguer–Lambert–Beer law in radiometry. However, that answer, completely determined by the mean-free-path (MFP), applies only to strictly uniform media.

A recent series of publications addressing this fundamental issue have provoked some controversy about non-exponential transmission laws, largely because of the unconventional description of the propagation part of transport problem in terms of "discrete-point process" theory rather than the traditional "continuum" theory encapsulated in the linear Boltzmann equation. Introducing discrete-point process modeling into transport through heterogeneous media, Kostinski [23] argued strongly that the presence of spatial correlations in *statistically* homogeneous media will invariably lead to sub-exponential behavior in the law of direct transmission. His findings were critiqued by Borovoi [24] who relied on classic continuum theory. In his reply, Kostinski [25] insists that the discrete-point approach is more fundamental and, to rest his case, he claims that transport in negatively correlated (a.k.a. "super-homogeneous") media can be modeled by discrete-point methods but *not* by continuum methods, pointing to a more detailed study by Shaw et al. [26]. One of the present authors weighed in very strongly favoring non-exponential mean transmission laws for *positively* correlated media using mainstream/continuum-based radiation transport theory [15]. This leaves

[2] See http://en.wikipedia.org/wiki/Pebble_bed_reactor, or http://www.cd-adapco.com/press_room/case_studies/060118_pebblebed.html for more information.

[3] These statistics are of immediate interest for stochastic RT in binary Markovian media.

the issue of negatively correlated media open to debate—one that we resolve in the course of the present investigation (cf. Section 5.2). We will present evidence that the two approaches are, in this respect at least, equivalent as long as the continuum notion of material particle density is appropriately broadened.

While this somewhat technical controversy unfolds, non-exponential transmission laws are finding their way into mean-field transport theories driven by specific applications. For instance, Davis [16] constructs a new 1D transport equation in integral form with anisotropic multiple scattering and calls the theory "anomalous transport" since it leads to asymptotic behavior captured by anomalous *diffusion* theory [14,27]. This new transport theory successfully explained then recent ground-based observations of time-domain RT in the Earth's cloudy atmosphere [28, and references therein]. As another example, Larsen [29] proposes a "non-classical" transport equation in integro-differential form that allows for non-exponential transmission laws by introducing a form of spatial memory between each scattering event. He furthermore derives by way of a careful asymptotic analysis a homogenized (but otherwise standard) diffusion theory that accounts for deviations of the mean transmission law from the exponential case; see also the paper by Larsen and Vasques [30] in this Special Issue. A spatially anisotropic generalization of this modeling framework has since been developed and applied to transport in experimental nuclear reactors with a pebble-bed core [31].

In the following section, we pose the general problem of radiation transport in heterogeneous 3D media in integral form, highlighting the key role of the transmission factor, i.e., the propagation part of the linear transport kernel. In Section 3, we survey previous results on non-exponential transmission laws that follow directly from statistical analysis of the propagation kernel. In Section 4, the adopted spatial variability model is presented and its general properties are described. In Section 5, we derive the transmission laws for previously unexplored classes of media in the model space, including cases where the largest fluctuation amplitudes are at the highest frequencies, and we discuss some ramifications. We draw our conclusions and look into possible applications in Section 6.

2. 3D radiation transport: in integral formulation

Let $I(\vec{x},\vec{\Omega})$ denote steady-state radiance at position $\vec{x}$ in 3D space propagating into direction $\vec{\Omega}$; its physical units are $\mathrm{W/m^2/sr}$(/μm, as needed). In monochromatic 3D RT, or one-group neutron transport, we seek to determine $I(\vec{x},\vec{\Omega})$ in a convex region $\mathrm{M} \subseteq \mathbb{R}^3$ (boundary $\partial\mathrm{M}$) where material properties are defined by (i) the extinction coefficient $\sigma(\vec{x})$ for either scattering or absorption or, in the case of neutrons, multiplication; (ii) the differential scattering cross-section (per unit volume) $\mathrm{d}\sigma_s/\mathrm{d}\vec{\Omega}(\vec{x};\vec{\Omega}'\to\vec{\Omega})$. Moreover, we are given the distributions of primary volume sources $(q_\mathrm{v}(\vec{x},\vec{\Omega}),\vec{x}\in\mathrm{M})$ and boundary sources $(q_\mathrm{b}(\vec{x},\vec{\Omega}),\ \vec{x}\in\partial\mathrm{M},\ \vec{\Omega}\cdot\hat{\mathbf{n}}(\vec{x})<0$ where $\hat{\mathbf{n}}(\vec{x})$ is the outward normal to $\partial\mathrm{M}$ at $\vec{x}$).

A convenient way of determining the linear transport problem at hand is to use the integral equation, particularly with numerical solutions in mind. It reads as

$$I(\vec{x},\vec{\Omega}) = \int_0^{s_{\partial\mathrm{M}}(\vec{x},-\vec{\Omega})} \mathrm{e}^{-\int_0^{s'}\sigma(\vec{x}-\vec{\Omega}s'')\,\mathrm{d}s''} \times\left[\int_{4\pi}\frac{\mathrm{d}\sigma_s}{\mathrm{d}\vec{\Omega}}(\vec{x}-\vec{\Omega}s';\vec{\Omega}'\to\vec{\Omega})I(\vec{x}-\vec{\Omega}s',\vec{\Omega}')\mathrm{d}\vec{\Omega}'\right]\mathrm{d}s' + Q(\vec{x},\vec{\Omega}) \tag{1}$$

where $s_{\partial\mathrm{M}}(\vec{x},-\vec{\Omega})$ is the distance along the upwind beam $\{\vec{x},-\vec{\Omega}\}$ from $\vec{x}$ to its unique intersection with $\partial\mathrm{M}$, assumed for simplicity to be absorbing (as opposed to partially reflective[4]). The integral source term denoted by $Q(\vec{x},\vec{\Omega})$ in the above can be computed from given volume- and boundary-source distributions:

$$Q(\vec{x},\vec{\Omega}) = \int_0^{s_{\partial\mathrm{M}}(\vec{x},-\vec{\Omega})} q_\mathrm{v}(\vec{x}-\vec{\Omega}s)\mathrm{e}^{-\int_0^{s}\sigma(\vec{x}-\vec{\Omega}s')\,\mathrm{d}s'}\,\mathrm{d}s + q_\mathrm{b}(\vec{x}-\vec{\Omega}s_{\partial\mathrm{M}}(\vec{x},-\vec{\Omega}))\mathrm{e}^{-\int_0^{s_{\partial\mathrm{M}}(\vec{x},-\vec{\Omega})}\sigma(\vec{x}-\vec{\Omega}s)\,\mathrm{d}s}. \tag{2}$$

In atmospheric radiation transport, M is most often taken to be a plane-parallel slab $\{\vec{x}\in\mathbb{R}^3; 0<z<L\}$ where L is the slab thickness; $q_\mathrm{v}(\vec{x},\vec{\Omega})$ would be used to model *isotropic* thermal sources inside the medium while $q_\mathrm{b}(\vec{x},\vec{\Omega})$ would be used to specify *isotropic* thermal emission by the underlying surface. In the solar spectrum, $q_\mathrm{b}(\vec{x},\vec{\Omega})$ would capture the *unidirectional* solar irradiation at the top of the medium while $q_\mathrm{v}\equiv 0$. Alternatively, one can usefully limit $I(\vec{x},\vec{\Omega})$ to once-or-more scattered radiation; boundary sources then vanish, and one uses the *anisotropic* volume source term[5]

$$q_\mathrm{v}(\vec{x},\vec{\Omega}) = F_0\frac{\mathrm{d}\sigma_s}{\mathrm{d}\vec{\Omega}}(\vec{x};\vec{\Omega}_0\to\vec{\Omega})\mathrm{e}^{-\int_0^{s_{\partial\mathrm{M}}(\vec{x},-\vec{\Omega}_0)}\sigma(\vec{x}-\vec{\Omega}_0 s)\mathrm{d}s}, \tag{3}$$

where F_0 is the solar constant at the wavelength of interest (in $\mathrm{W/m^2/\mu m}$) and $\vec{\Omega}_0$ is the direction of incidence of the solar beam.

For the present study, the important fact about (1)–(3) is the recurring appearance of

$$T(\vec{x}_0,\vec{\Omega};s) = \mathrm{e}^{-\int_0^{s}\sigma(\vec{x}_0+\vec{\Omega}s')\,\mathrm{d}s'}, \tag{4}$$

which is the *local* law of direct transmission from $\vec{x}_0$ to $\vec{x}_1 = \vec{x}_0+\vec{\Omega}s$, i.e., over distance $s=\|\vec{x}_1-\vec{x}_0\|$ along $\vec{\Omega}=(\vec{x}_1-\vec{x}_0)/\|\vec{x}_1-\vec{x}_0\|$. From a Monte Carlo standpoint, this is the cumulative probability for the random distance from $\vec{x}_0$ to the next scattering or absorption event along $\vec{\Omega}$ to exceed s. In kinetic-theoretical terms, it is the probability of particles leaving $\vec{x}_0$ to reach $\vec{x}_1$ uncollided.

In stochastic media, $T(\vec{x}_0,\vec{\Omega};s)$ or, equivalently,

$$T(\vec{x}_0,\vec{x}_1) = \mathrm{e}^{-\overline{\sigma}(\vec{x}_0,\vec{x}_1)\|\vec{x}_1-\vec{x}_0\|}, \overline{\sigma}(\vec{x}_0,\vec{x}_1) = \int_0^1 \sigma(u\vec{x}_0+(1-u)\vec{x}_1)\,\mathrm{d}u \tag{5}$$

is a critically important non-local quantity. The segment-averaged extinction $\overline{\sigma}(\vec{x}_0,\vec{x}_1)$, hence $T(\vec{x}_0,\vec{x}_1)$, are random variables. We are therefore keenly interested in the statistical properties of $T(\vec{x}_0,\vec{x}_1)$. This is indeed the crucial

[4] Bi-directional reflection by boundary elements can in fact be modeled as a special kind of scattering—the term in square brackets in (1). So the integral equation in (1) is a quite general formulation of linear transport problems.

[5] This results from setting $q_\mathrm{v}\equiv 0$, $q_\mathrm{b}(\vec{x},\vec{\Omega}) = F_0\delta(\vec{\Omega}-\vec{\Omega}_0)$ on the illuminated subset of M (i.e., $\{\vec{x}\in\mathrm{M};\vec{\Omega}_0\cdot\hat{\mathbf{n}}(\vec{x})<0\}$), and 0 elsewhere; then once iterating (1) and (2), starting with $I_0\equiv q_\mathrm{b}$.

propagation part of the linear transport kernel in (1) that remains even when the scattering is everywhere isotropic, as it is sometimes assumed in neutron transport theory for simplicity (i.e., $\mathrm{d}\sigma_s/\mathrm{d}\vec{\Omega}(\vec{x};\vec{\Omega}'\to\vec{\Omega}) \equiv \sigma_s(\vec{x})/4\pi$).

3. Mean transmission law: exponential or not?

We will focus on the ensemble-average value of $T(\vec{x}_0,\vec{x}_1)$, which we denote $\langle T(s)\rangle$, letting $\langle\cdots\rangle$ denote ensemble averages. This is a spatial statistic that will depend strongly on the nature of the correlations in the random optical medium. At least in *statistically* homogeneous and isotropic media, it will depend only on the transport distance $s=\|\vec{x}_1-\vec{x}_0\|$, an assumption we will make for simplicity in the present study.[6]

3.1. The case of functions

Davis and Marshak [15] investigated the properties of $\langle T(s)\rangle$ under very general assumptions about the variability of $\sigma(\vec{x})$. In essence, they only assumed that the natural notation "$\sigma(\vec{x})$" makes mathematical sense, in other words, that σ is a well-defined function of position $\vec{x}$. It need not be a very well-behaved function since all that is required is a degree of continuity. In particular, differentiability is *not* required. This is a good thing since we will see further on that continuous but non-differentiable functions are well-suited for describing the turbulent structure of real clouds, as observed by airborne in situ probes [33–36].

Elementary kinetic theory tells us that σ is the density of material particles in the media times their total (scattering+absorption) microscopic cross-section. Assuming all the material and transported particles have the same microscopic cross-sections, the spatial variability of σ just reflects that of the material density.[7] Now, density is a continuum notion that requires a specific connection between finite numbers of particles in varying volumes around $\vec{x}$. Specifically, we naively require that

$$\overline{\sigma}_r(\vec{x}) = \frac{1}{4\pi r^3/3}\iiint_{\|\vec{x}'-\vec{x}\|<r} \sigma(\vec{x}')\,\mathrm{d}\vec{x}' \tag{6}$$

does not depend on r, if small enough, and we denote this value $\overline{\sigma}_0(\vec{x})$. This should hold at least to within the Poissonian[8] fluctuations to be expected when the volume's dimensions become commensurate with the inter-particle distance for the material of interest. In the same spirit, we ask that

$$\overline{\sigma}(\vec{x},\vec{x}+\vec{\Omega}r) = \frac{1}{r}\int_0^r \sigma(\vec{x}+\vec{\Omega}s)\,\mathrm{d}s \approx \overline{\sigma}_0(\vec{x}) \tag{7}$$

for any choice of $\vec{\Omega}$ when r is small enough. Davis and Marshak called this presumably benign property of the medium "one-point scale-independence."

Three general results for one-point scale-independent media were then derived in [15]:

- The mean direct transmission law $\langle T(s)\rangle$ is exponential only if $\sigma(\vec{x})$ is uniform in M. This is the non-trivial converse of the elementary result showing that, if σ is uniform, then $T(s)=\exp(-\sigma s)$.
- Recalling that the ensemble-average free-path distribution is $p(s)=|\mathrm{d}\langle T\rangle/\mathrm{d}s|$, the actual (ensemble-average) MFP given by $\langle T(s)\rangle$; specifically, we compute $\ell = \mathcal{E}(s)=\int_0^\infty sp(s)\,\mathrm{d}s$ and find that ℓ is always larger than $1/\langle\sigma\rangle$, the logical prediction from the exponential distribution when one only knows the mean extinction. Conversely, $\ell=1/\langle\sigma\rangle$ only in uniform media.
- $\langle T(s)\rangle$ is always sub-exponential in the sense that, if one uses the above MFP ℓ to predict higher order moments $\mathcal{E}(s^q)=\int_0^\infty s^q p(s)\,\mathrm{d}s$ for q = 2,3,…, then the exponential assumption yields an underestimate. In other words, $\mathcal{E}(s^q)\geq q!\ell^q$ for $q>1$, where "=" applies only when the medium is uniform.

This last item is fundamentally a statement about the tail of the free-path distribution, that is, how $\langle T(s)\rangle$ decays as $s\to\infty$. All of the above results follow from Jensen's inequality [38] as applied in various ways to convex functions of σ and of s.

3.2. Extension to measures

The present study is about relaxing the assumption of one-point scale-independence. This generalization is possible, but the price is that we can no longer think of σ as a *regular* function, that is, with some form of continuity almost everywhere, hence has a well-defined numerical value at almost every point in M. Since it only appears under line integrals in (1) and (2), we can safely state that σ only needs to be a *measurable* function, or simply a *measure* on M.

A prime example of a measure is Dirac's delta "function" $\delta(x)$, actually a distribution in the sense of Schwartz [39]. It is generally described as being 0 everywhere except at x = 0 where it is ∞ …in such as way that $\int_{-\infty}^{+\infty}\delta(x)\,\mathrm{d}x=1$. More rigorous definitions do not attempt to write it outside of an integral: $\int_{-\infty}^{+\infty}\delta(x-y)f(x)\,\mathrm{d}x=f(y)$, for a vast class of test functions f. Physicists sometimes define $\delta(x)$ as a singular limit of vanishingly narrow functions (e.g., Gaussians or piecewise-constant functions) that integrate to unity. Mathematicians tend to use measure-theoretic language: $\int_a^b\delta(x)\,\mathrm{d}x=1$ if $a<0<b$, and 0 otherwise.

There have already been investigations of RT in very sparse optical media represented by measures that patently violate the one-point scale-invariance property in (7). In media with a fractal *internal* structure, the coarse-scale extinction $\overline{\sigma}_r(\vec{x})$ in (6) will vary, presumably like the estimate of the local mean material density, as $r^{-3+\alpha(\vec{x})}$ where $\alpha(\vec{x})$ is the prevailing "regularity" exponent varying between 0 (e.g., when $\sigma(\vec{x})\propto\delta(\vec{x})$) and 3 (an exponent-based

[6] Fundamentally, this reduces to the initial value problem for a stochastic ODE with *multiplicative* noise: $\mathrm{d}T/\mathrm{d}s=-\sigma(s)T$, $s\geq 0$, $T(0)$ = 1; see [32] for many examples and applications.

[7] If cross-sections vary from particle to particle (as, e.g., cloud particles with polydisperse sizes), then one uses the cross-section averaged over the particle population. The assumption that such an average is always meaningful has, however, been questioned, particularly when it comes to the largest particles because they are so rare [37].

[8] As discussed elsewhere in this article, Kostinski [23] questions this assumption and describes the ramifications for photon propagation.

statement of the one-point scale-invariance property as used, e.g., in turbulence theory [40]).

In this context, Davis et al. [41] obtained an analytical expression for the domain-average direct transmission through a deterministic 2D fractal, the Sierpiński sieve [42], in the form of a power-law in mean optical depth. Knyazikhin et al. [43] independently studied the propagation of light through fractal structures representative of vegetation canopies; they modeled the ray-canopy intersection as a Cantor-like set [42], again finding power-law statistics for the probability of uncollided survival. This finding was later interpreted as a "missing solution" [44], a process not captured by the standard RT model where the canopy is likened to a turbid medium. Beyond these 0th-order scattering studies, Watson et al. [45] have recently examined single scattering responses.

Multiple scattering in sparse fractal media was addressed two decades ago by Lovejoy, Gabriel, Davis et al. [1,46,47], using both analytical and computational techniques, with terrestrial clouds in mind. In the absence of absorption, they found that total (direct+diffuse) transmission goes as a power-law in mean optical depth ($\overline{T} \sim 1/\overline{\tau}^{\nu}$) that is weaker ($\nu < 1$) than for uniform media (where $\nu = 1$). This result, based on a deterministic monofractal model, was soon generalized to random multifractal media with log-normal statistics [48]. Multiple scattering studies in such sparse stochastic media are ongoing: Lovejoy et al. [49] recently examined log-Lévy multifractals in considerable detail.

Finally, as reminded further on, the internal structure of real clouds (as defined by the condensed water density in g/kg as well as for extinction) is akin to the fluctuations of an admixture in a turbulent flow. In particular, $k^{-5/3}$ wavenumber spectra are observed, whereas sparse fractal distributions have much smaller spectral exponents ($k^{-\beta}$ with $0 \le \beta < 1$). Consequently, cloudy airmasses are one-point scale-invariant optical media, even though their boundaries are notoriously fractal [50,51]. Nonetheless, the largest cloud droplets are found, as one intuitively expects, in increasingly sparse volumes as the radius increases. Based on extensive cloud microphysical data collected by aircraft along linear transects through clouds, there is empirical evidence that the largest particles tend to cluster more than expected for random Poissonian fluctuations [37]. More to the present point, there are non-negligible radiative ramifications of this clustering, particularly for bulk absorption in the cloud [52].

In the remainder of this paper, we extend RT (starting with the propagation kernel) to yet another class of measures that are akin to different flavors of noise. For simplicity, and leading to insights from analytical results, these random measures are assumed to have Gaussian one-point statistics and monofractal scaling properties, but this is not essential to the conclusions.

4. Adopted variability model

In the remainder, the extinction field is defined as a random measure denoted "$\sigma(x)\,\mathrm{d}x$" with the understanding that, under general circumstances, the two terms must be kept together; alternatively, we use the Stieltjes notation "$\mathrm{d}\tau(x)$" for the corresponding element of *optical* distance. Leaving a completely general approach for future work, we concentrate here on a representative and relevant class of stochastic optical media that has two components: (1) a regular, indeed constant, part $\langle \sigma \rangle$ that is strictly positive, and (2) a noise that we take as Gaussian with zero mean and fluctuations that are scale-invariant in the sense that their Fourier amplitudes follow a power-law trend in wavenumber k. We recall that, in general, only definite integrals of $\mathrm{d}\tau(x)$ have well-defined numerical values for this type of fluctuating medium. In other words, we can only evaluate quantities such as

$$\tau(x_0,x_1) = \int_{x_0}^{x_1} \mathrm{d}\tau(x), \tag{8}$$

that we interpret in the sense of Lebesgue [53], as well as Fourier integrals. In the present context, we identify this random variable with optical distance $\int_{x_0}^{x_1} \sigma(x)\,\mathrm{d}x$ that appears multiple times in the integral transport equation set (1)–(3) in a notation that is usually understood as a standard Riemann integral.

4.1. Formal definition in Fourier space

The model is best defined in Fourier space where, because of (7), we can work in 1D without loss of generality. Letting $k \in \mathbb{R}$ denote wavenumber, the energy spectrum of the 1D measure σ is also a measure. In the present model, it is defined (up to a multiplicative factor) as

$$E_\sigma(k)\,\mathrm{d}k = |\hat{\sigma}(k)\,\mathrm{d}k|^2 \sim |k|^{-\beta}\,\mathrm{d}k \tag{9}$$

for $k \neq 0$, a value we deal with further on. The spectral exponent β is usually assumed positive, but there is no fundamental reason it cannot be negative as well. To keep variance ($= 2\int_{0^+}^{\infty} E_\sigma(k)\,\mathrm{d}k$) finite, k in (9) will have at least one cutoff value: $k_L = 1/L > 0$ (where L is the *finite* outer scale), $k_{\mathrm{Nyq}} = 1/2\Delta x < \infty$ (Nyquist wavenumber, where Δx is the *finite* inner scale), or both (in which case we assume the number of samples $L/\Delta x = 2k_{\mathrm{N}}/k_L \gg 1$). At a minimum, $k_L > 0$ if $\beta \ge 1$ to avoid the so-called "infrared" catastrophe (variance $\to \infty$) and/or $k_{\mathrm{Nyq}} < \infty$ if $\beta \le 1$ to avoid the so-called "ultraviolet" catastrophe. In numerical implementations, both divergences are naturally avoided since the number of spatial samples $N_{\mathrm{pts}} = L/\Delta x$ will be large but finite.

Letting $\mathrm{i} = \sqrt{-1}$, we thus assume

$$\begin{aligned}\hat{\sigma}(k)\,\mathrm{d}k = \mathrm{F}[\sigma]\,\mathrm{d}k &= \mathrm{d}k \int_{-\infty}^{+\infty} \mathrm{e}^{+\mathrm{i}kx}\,\mathrm{d}\tau(x) \\ &= \text{constant } \times k^{-\beta/2} g_k \mathrm{e}^{\mathrm{i}\phi_k}\sqrt{\mathrm{d}k}\end{aligned} \tag{10}$$

for $k > 0$, and $\hat{\sigma}(0)\,\mathrm{d}k = \langle \sigma \rangle\,\mathrm{d}k$; for $k < 0$, we take the complex conjugate of (10) to ensure a real-valued inverse Fourier transform. In the above, g_k denotes a zero-mean/unit-variance Gaussian random amplitude $N(0,1)$ for the Fourier mode. We have introduced here the notation

$$N(\mu,\text{std.dev.}),\text{std.dev.} = \sqrt{\text{variance}}$$

for a Gaussian random variable with mean and standard deviation in the 1st and 2nd arguments, respectively, and ϕ_k is a uniform random phase in $[0,2\pi)$. The exponent β defines the scaling property, with qualitative ramifications

discussed in the next subsection, while the constant in (10) is an overall variability strength parameter that will be specified implicitly further on, bearing in mind the following constraint. In the present application, we will tune the maximum recommended value for the constant in (10) as a function of $\langle\sigma\rangle$ and β in such a way that keeps the definite integrals of

$$\mathrm{d}\tau(x)=\sigma(x)\,\mathrm{d}x=\mathrm{F}^{-1}[\hat{\sigma}]\,\mathrm{d}x=\frac{\mathrm{d}x}{2\pi}\int_{-\infty}^{+\infty}\mathrm{e}^{-\mathrm{i}kx}\hat{\sigma}(k)\,\mathrm{d}k \tag{11}$$

in (8) non-negative for a vast majority of possible positions x, integration domains, and realizations of $g_k\mathrm{e}^{\mathrm{i}\phi_k}(k>0)$. Within the Gaussian framework, one cannot ask for more.

One practical algorithm for numerical implementations (where $\mathrm{d}x=\Delta x$ and $\mathrm{d}k = 1/L$) is to decide on a value for N_{pts}, then fix the variability β in (10), leaving the constant as unity. Then, one performs the inverse (fast) Fourier transform in (11) assuming $\hat{\sigma}(0)\,\mathrm{d}k=0$. Then seek the minimum of the outcome $\sigma(x)\Delta x$, a necessarily negative number. Subtracting and then dividing the outcome by this number yields an acceptable realization of $\sigma(x)\Delta x$ normalized by its mean $\langle\sigma(x)\Delta x\rangle$, which is itself independent of x (statistical homogeneity). However, this last procedure is only for generating illustrations since it couples two free parameters of the model, the mean and amplitude of the fluctuations. When both are set independently, at least some realizations will have negative values. This is necessary to generate truly Gaussian statistics.

Fig. 1 shows one realization each for the choices $\beta=-1$, 0, 1, 5/3, and 3 using the above algorithm for N_{pts} = 1024. The same sequence of Gaussian random variable g_k and random phases ϕ_k was used for $k>0$ in (10) with all selected values of β; only the Fourier mode amplitudes were changed according to (9). That explains the similarity in overall shape of the fields with the largest β values.

4.2. Nomenclature

Beyond the large-scale mean value, the adopted model for the extinction field in (10) and (11) has two variability parameters: (1) a multiplicative prefactor that controls the amplitude of the 1-point Gaussian PDF; (2) spectral scaling exponent β that determines 2-point (spatial correlation) statistics. Qualitative differences occur as β is varied, from large to small values:

1. for $\beta\geq 3$, every realization of $\sigma(x)$ is a random but smooth (almost everywhere differentiable) function with, in particular, no discontinuities (otherwise β jumps to 2);
2. for $2<\beta<3$, σ is a fractional Brownian motion (fBm) with "persistence" in the sense that $\langle[\sigma(x+2r)-\sigma(x+r)][\sigma(x+r)-\sigma(x)]\rangle>0$ for any two successive increments at any scale r [42];
3. for $\beta=2$, σ is the spatial counterpart of classic Brownian motion (Bm, a.k.a. Weiner–Lévy process), where successive increments at any scale are independent, i.e., $\langle[\sigma(x+2r)-\sigma(x+r)][\sigma(x+r)-\sigma(x)]\rangle=0$;
4. for $1<\beta<2$, σ is a fBm with "anti-persistence" in the sense that $\langle[\sigma(x+2r)-\sigma(x+r)][\sigma(x+r)-\sigma(x)]\rangle<0$ for two successive increments at scale r, a scenario of tremendous interest in turbulent media [54] such as clouds;
5. for $\beta=1$, we have the special case of spatial "$1/f$" (a.k.a. "red") noise, borrowing the traditional time-domain notation, that is on the cusp between the above random fields with diverging variance due to large-r/small-k behavior (the infrared catastrophe) and the following ones where the divergence is at small-r/large-k's (the ultraviolet catastrophe);
6. for $0<\beta<1$, σ is a field of "pink" noise that generates persistent fBm by integration (in practice, a division by ik in Fourier space);
7. for $\beta=0$, σ is a field of "white" noise that generates standard Bm by integration;
8. for $-1<\beta<0$, σ is a field of "blue" noise that generates anti-persistent fBm by integration.

The noted connection, via definite integrals, between the stationary Gaussian scaling noises and the non-stationary fBm processes proves crucial in the following analysis of systematic transport effects.

From a stochastic modeling perspective, the $\beta=1$ case is a critical threshold between statistically stationary fields when β is smaller and non-stationary ones for β larger than unity [42]. A visual distinction between the stationary processes in the top panels and the non-stationary ones at the bottom is the density of zero/mean-level crossings in Fig. 1: they are very frequent for stationary cases, quite rare for non-stationary ones. Therefore, from a practical data analysis perspective, a sequential sample of a stationary process will quickly converge to their one-point statistics such as mean, variance, etc., while a non-stationary one can take forever in the sense that one may run out of data before even low-order moments have stabilized; see illustration with cloud probe data in [34].

One should actually talk about statistically *homogeneous* random functions since they unfold in space rather than time, but we will carry on with this wide-spread abuse of the time-domain language. Also throughout this study, we think of stationarity in the "broad" sense, meaning based solely on 1st- and 2nd-order moments and spatial statistics.

4.3. Important statistical properties

The Wiener–Khinchin theorem states that, for any broad-sense stationary process $f(x)$, energy spectrum $E_f(k)$ and autocorrelation function form a Fourier transform pair [55, among others]. The autocorrelation function is defined as

$$G_f(r)=\langle[f(x+r)-\langle f\rangle][f(x)-\langle f\rangle]\rangle=\langle f(x+r)f(x)\rangle-\langle f\rangle^2, \tag{12}$$

independently of x since f is a stationary random process, and we note that $G_f(0)=\langle[f(x)-\langle f\rangle]^2\rangle$ is the 1-point variance. For extinction fields based on scaling stationary noises, this tells us that a wavenumber spectrum with a power-law decay in $0<\beta<1$ leads to a power-law autocorrelation function

$$G_\sigma(r)\sim r^{-\gamma}, \tag{13}$$

where

$$\gamma=1-\beta, \tag{14}$$

so we also have $0<\gamma<1$.

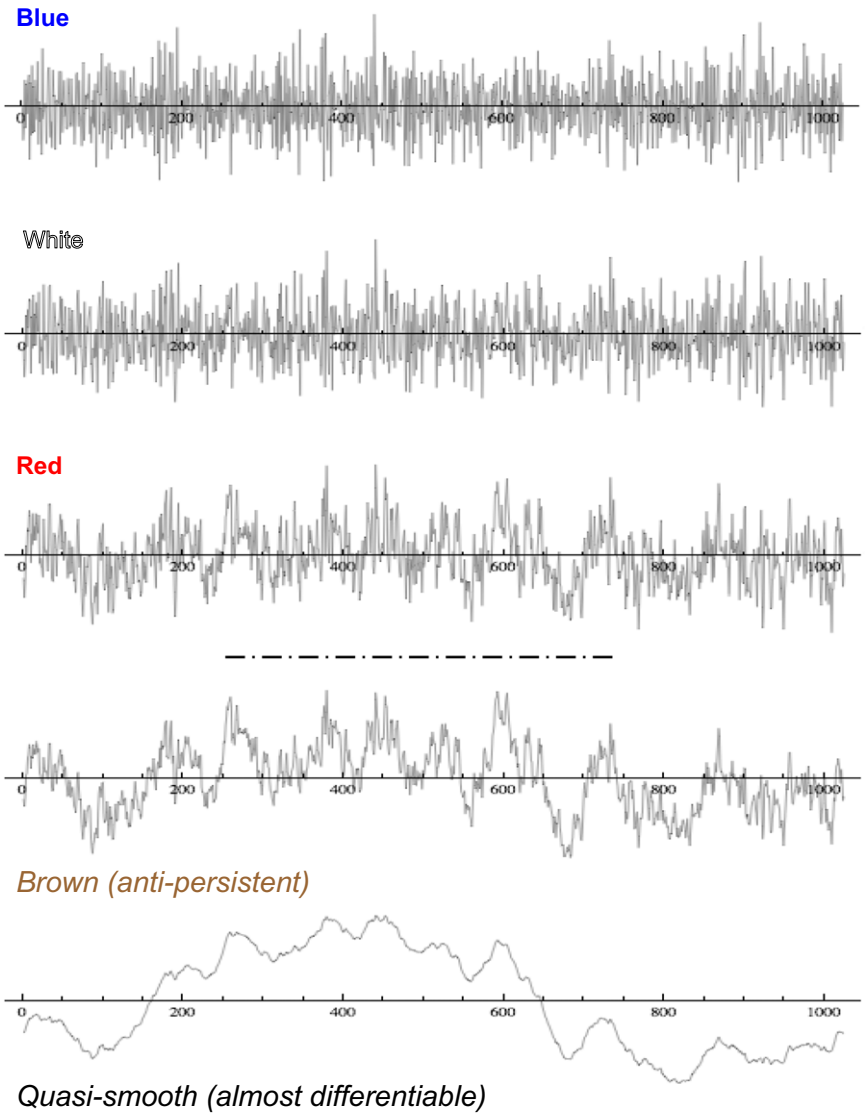

Fig. 1. Simulated examples of extinction transects $\sigma(x)\Delta x$ through random optical media with power-law wavenumber spectra (1024 samples, in arbitrary units, with $\Delta x = 1$); more precisely, for the top three cases, we plot $\overline{\sigma}(x)\Delta x$ using a 1D counterpart of (7). From top to bottom: $\beta = -1, 0, 1, 5/3, 3$; respectively: blue, white, red, and brown noises, followed by an almost everywhere differentiable function. Eq. (11) was used to generate these fields by inverse fast Fourier transformation. (For interpretation of the references to color in this figure legend, the reader is referred to the web version of this article.)

The limit $\beta \to 0^+$, hence $\gamma \to 1^-$, leads to the well-known case of white noise where the Wiener–Khinchin theorem gives us $\delta(r)$ on the r.-h. side of (12): white noise is indeed $\delta-$correlated. The limit $\beta \to 1^-$, hence $\gamma \to 0^+$, leads to a $G_\sigma(r)$ that does not decay with distance r, thus marking passage into the realm of random functions with "long-range" memory, that is, any realization of $\sigma(x)$ with $\beta > 1$.

The Wiener–Khinchin theorem for non-stationary processes, but with stationary increments, tells us the energy spectrum and the (2nd-order) structure function form a Fourier transform pair [56, among others]. In general, the q th-order structure function is defined as

$$\mathrm{SF}_f(q,r) = \langle [f(x+r) - f(x)]^q \rangle, \tag{15}$$

independently of x since f has stationary increments, also known as the variogram. We note that $\mathrm{SF}_f(2,r) = 2[G_f(0) - G_f(r)]$ in the case of broad-sense stationary processes. For extinction fields based on scaling non-stationary processes, Wiener–Khinchin tells us that a wavenumber spectrum with a power-law decay in $1 < \beta < 3$ leads to a 2nd-order structure function

$$\mathrm{SF}_\sigma(2,r) \sim r^{2H_\beta}, \tag{16}$$

where[9]

$$H_\beta = \frac{\beta - 1}{2} \tag{17}$$

[9] In the fractal literature, where physical-space methods are often favored, one often sees the converse: β is given by $2H_\beta + 1$, e.g., Mandelbrot [42].

is known as the Hurst exponent [42]. We therefore have $0 < H_\beta < 1$. We note that, in this $(1 < \beta < 3)$ regime, $\sigma(x)$ is a valid notation since it is a regular function that is at least stochastically continuous. In other words, we have $\mathrm{SF}_\sigma(2,r) \to 0$ when $r \to 0$.

As anticipated above, we see that the limit $\beta \to 3$ (hence $H_\beta \to 1$) leads to smooth/differentiable behavior for $\sigma(x)$, specifically, $|\sigma(x+r)-\sigma(x)| \sim r$ at typical (if not all) points. We also note that (15) and (16) can be combined to show that

$$\langle [\sigma(x+2r)-\sigma(x+r)][\sigma(x+r)-\sigma(x)] \rangle = \mathrm{SF}_\sigma(2,2r)/2 - 2\mathrm{SF}_\sigma(2,r) \sim (2^{2H_\beta-1}-1) \times r^{2H_\beta}. \tag{18}$$

This justifies the sign convention used in Section 4.2 to describe the correlations between two successive increments in $\sigma(x)$ at scale r.

Finally, the statistical property expressed in (15) and (16) has a *local* version:

$$|\sigma(x+r)-\sigma(x)| \sim r^{h(x)}, \tag{19}$$

where $h(x)$ is the local regularity (a.k.a. Hölder) exponent [40]. From a multi-resolution analysis perspective [57], we see that (7) is in essence a local constraint on the projection of $\sigma(x)$ onto the so-called "scaling" function (a local *coarse* value at scale r). By the same token, (19) is a constraint on the projection of $\sigma(x)$ onto the so-called "wavelet" function (local *detail* at scale r). It is clear that, for one-point scale-independence (a coarsening property) to prevail, we need the detailed behavior to be characterized by $h(x) > 0$. In contrast, any discontinuity at x leads to $h(x) \le 0$.

In the remainder of this paper, we are concerned only with noises, $\beta \le 1$ (cases 6–8 in Section 4.2). All cases with $\beta > 1$ have continuity and were treated by Davis and Marshak [15]. However, we will exploit the correspondence (through Lebesgue integration) between a noise characterized by $|\beta| \le 1$ and a fBm with a spectral exponent $\beta+2$, hence a Hurst exponent $H_{\beta+2} = (\beta+1)/2$ from (17).

5. Mean transmission laws for unexplored model space

5.1. Media represented by red, pink and white noises $(0 \le \beta \le 1)$

We are first interested in computing the mean transmission law[10]

$$\langle T(x_0,x_1) \rangle = \langle \exp[-\tau(x_0,x_1)] \rangle, \tag{20}$$

from (8), as a function of propagation distance $s = |x_1 - x_0|$ for the above class of models based on scaling noises, but only when $0 \le \beta \le 1$. Equivalently, we assume $1/2 \le H_{\beta+2} = (\beta+1)/2 \le 1$ in (17) for the associated Brownian motion $(\beta = 0)$ or *persistent* fBm $(0 < \beta < 1)$. This is an immediate extension of Davis and Marshak's 2004 paper [15] on 3D optical media with $\beta > 1$ in our present notation.[11]

Fig. 2 shows three fields for one realization. In the top panel, we see $\sigma(x)$ as in the middle panel of Fig. 1 but a different realization of the red noise $(\beta = 1)$ case, this time normalized by $\langle \sigma \rangle$. The value of the constant in (10) is chose close to the maximum value for the given $\langle \sigma \rangle$ and β. Consequently, the most extreme negative fluctuation of $\sigma(x)\Delta x$ is ≈ 0. The corresponding $\tau(0,x)$ is plotted in the middle panel for the case where $\langle \tau(0,L) \rangle = \langle \sigma \rangle L = 5$. Finally, in the bottom panel, we have $T(0,x)$, the quantity that is actually averaged to form $\langle T(s) \rangle \equiv \langle T(0,x) \rangle|_{x=s}$ by stationarity.

More specifically, we wish to evaluate

$$\langle T(s) \rangle = \langle \mathrm{e}^{-\tau} \rangle(s) = \int_0^\infty \mathrm{e}^{-\tau} \Pr\{\tau, \mathrm{d}\tau | s\}, \tag{21}$$

where $\Pr\{\tau, \mathrm{d}\tau | s\}$ is the probability law for the random variable τ in (8) and (20) for fixed s, viewed here as a fixed parameter. We now note that the definite integral $\tau(x_0,x_1)$ of scaling noise is simply an increment of the associated fBm, and we know what its distribution is. It is normally distributed with mean value $\langle \sigma \rangle s$ and variance given by $\mathrm{SF}_\sigma(2,s)$ in (15) and (16). For specificity, we will write

$$\mathrm{SF}_\sigma(2,s) = C_\sigma^2 \times (\langle \sigma \rangle s)^{2H}. \tag{22}$$

Here, and in the remainder of the paper, $2H$ is short for $2H_{\beta+2} = \beta+1$ from (17). The non-dimensional parameter C_σ^2 is related to the constant in (10), recalling that its maximum value is determined by the values selected for $\langle \sigma \rangle$ and β (equivalently, H). In short, we have

$$\tau(x_0,x_1) \stackrel{\mathrm{d}}{=} N(\langle \sigma \rangle s, C_\sigma(\langle \sigma \rangle s)^H), \tag{23}$$

meaning "equal in distribution." As anticipated, we immediately see that this model of optical variability is somewhat flawed because the support of a Gaussian is all of $\mathbb{R}$ while $\tau(x_0,x_1)$ is necessarily positive on physical grounds. With this assumption about $\tau(x_0,x_1)$, $T(x_0,x_1)$ is a log-normal random variable, and we will have to mitigate the unphysical excursions to values in excess of unity.

Conveniently, we know how to compute the characteristic function of a Gaussian random variable, namely,

$$\langle \mathrm{e}^{+\mathrm{i}\xi N(\mu,\sqrt{\nu})} \rangle = \int_{-\infty}^{+\infty} \frac{\mathrm{e}^{-(N-\mu)^2/2\nu}}{\sqrt{2\pi\nu}} \exp(-\mathrm{i}\xi N)\,\mathrm{d}N = \exp(-\mathrm{i}\mu\xi - \nu\xi^2/2). \tag{24}$$

We use this as an approximate estimation of (21), the approximation being an extension of the integration limits from $(0,\infty)$ to $(-\infty,+\infty)$. As stated earlier, the impact of this extension to physically spurious negative values of τ is small if the assumed mean extinction $\langle \sigma \rangle$ is large enough, in view of the variability amplitude parameter C_σ. At any rate, we can control this adverse impact of the simplifying assumption of Gaussian variability.

[10] There is a *non-random* spectral analog of computing average values of $\mathrm{e}^{-\tau_\lambda}$, where λ is wavelength, over a spectral interval. In some spectral regions of atmospheric interest, τ_λ can vary so fast with ν that Riemann integration is not an option. This is due to spectrally dense highly quantized molecular absorption features. "Band model" approaches to this problem are, in essence, an implementation of Lebesgue integration theory; see, for instance, [58]. The energy dependence of nuclear cross-sections has similarly unwieldy behavior in resonance regions, and the practical solution for transport is the same.

[11] Davis and Marshak [15] in fact already treated (in physical space, using a finite inner scale) the $\beta = 0$ case of white noise/δ−correlated optical media, but this was just to provide a counterexample to their required one-point scale-independence property.

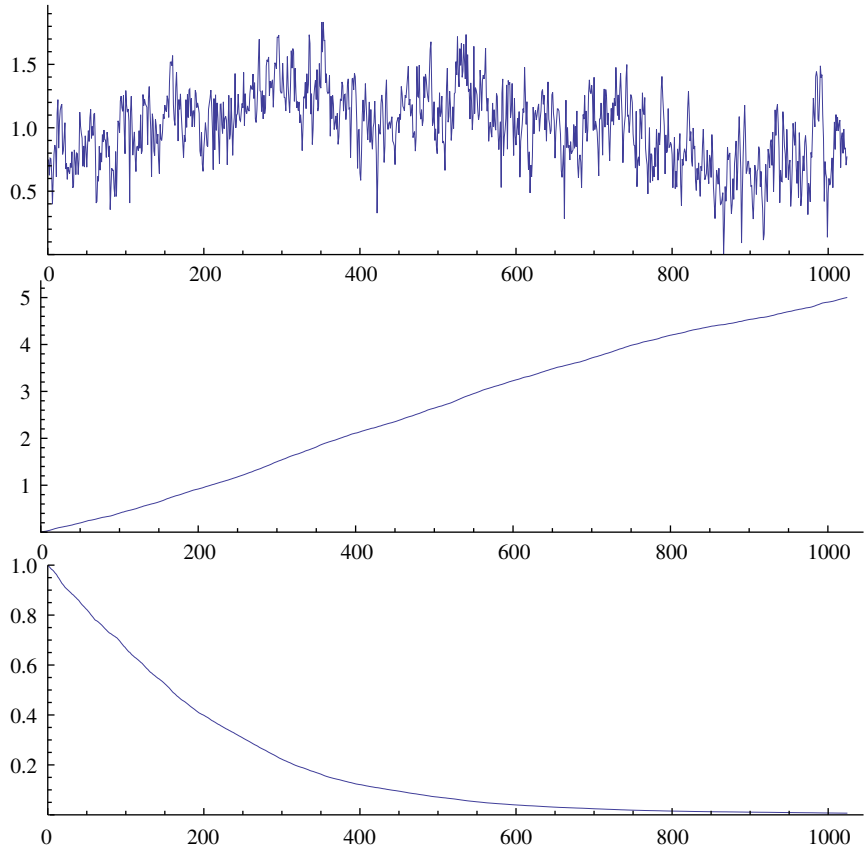

Fig. 2. *Top*: Another realization of the red noise ($\beta = 1, H = 0$) case in Fig. 1, middle panel; here, we plot $\sigma(x)/\langle\sigma\rangle$ versus sample position x running from 0 to L = 1024. *Middle:* Optical distance $\tau(0,x)$ from (8) versus x, assuming that $\langle\tau(0,L)\rangle = \langle\sigma\rangle L = 5$. *Bottom:* Direct transmittance $T(0,x)$, one element from the ensemble average in (20), versus x. (For interpretation of the references to color in this figure legend, the reader is referred to the web version of this article.)

Setting $\xi = \pm\mathrm{i}$ in (24), with $\mu = \langle\sigma\rangle s$ and $\nu = (C_\sigma\mu)^{2H}$, we obtain

$$\langle T(s)\rangle = \langle \mathrm{e}^{-\tau}\rangle(s) \approx \exp[-\langle\sigma\rangle s + (C_\sigma^2/2)\times(\langle\sigma\rangle s)^{2H}]. \quad (25)$$

This approximation will remain valid as long as $\langle\sigma\rangle$ is large enough (equivalently, C_σ is small enough) that we can find a useful range for the transport distance s where $\langle T\rangle(s) \le 1$ and $\mathrm{d}\langle T\rangle/\mathrm{d}s < 0$.

The special case of $\delta-$correlated fluctuating media with a Gaussian PDF is retrieved for H = 1/2, hence

$$\langle T(s)\rangle \approx \exp[-(1-C_\sigma^2/2)\times\langle\sigma\rangle s]. \quad (26)$$

As noted by Davis and Marshak [15], there is an effective ("homogenized") value of σ, smaller than the mean by a relative correction factor of $C_\sigma^2/2$ (which should obviously not exceed unity, hence $C_\sigma < \sqrt{2}$). This accounts for the raw variability in complete absence of spatial correlations. The fact that the homogenization is an exact result is unique to the Gaussian model. Others [19,59,60, etc.] have investigated $\langle \mathrm{e}^{-\tau}\rangle$ without any consideration of spatial correlations but using appropriately non-Gaussian PDFs for τ; they have invariably found nonlinear deviations (consistent with Jensen's inequality) to what would equate here with the mean trend $\langle\sigma\rangle s$.

Otherwise, for $H \neq 1/2$, we find a positive correction term to $-\langle\sigma\rangle s$ for $\ln\langle T(s)\rangle$: $C_\sigma^2(\langle\sigma\rangle s)^{2H}/2$, with $2H > 1$. This extends to pink-noise media Davis and Marshak's finding of sub-exponential transmission laws for what is denoted here as "$\beta > 1$" cases. In summary, one obtains sub-exponential tails for any $\beta > 0$ and exponential ones when $\beta = 0$, as well as when $C_\sigma^2 = 0$.

We note that when $H > 1/2$, the correction term in s^{2H} will eventually grow larger in magnitude than the presumably dominant term, $-\langle\sigma\rangle s$; the transport distance to this turn-around in $\langle T(s)\rangle$ is

$$s^\star = \frac{1/\langle\sigma\rangle}{(C_\sigma^2 H)^{1/(2H-1)}}, \quad (27)$$

where the numerator is the estimated MFP in the absence of variability. In reality, we never expect the derivative of $\langle T(s)\rangle$ to vanish at finite s—let alone start increasing with s and eventually exceed unity. This is clearly an artifact of the Gaussian assumption that becomes manifest at large values of s: persistent fluctuations of τ into negative values. In practice, we would never apply the model to such high values of s and/or C_σ. Specifically, we require for this regime that

$$(C_\sigma^2 H)^{1/(2H-1)} \ll 1, \quad (28)$$

and also that $s \ll s^\star$, thus maximized in (27).

5.2. Media represented by blue noises ($-1<\beta<0$)

The above computation of $\langle T(s)\rangle$ for $1/2\le H<1$ ($0\le\beta<1$) carries over wholesale to $0<H<1/2$ ($-1<\beta<0$); only the analysis of the results changes qualitatively. The fact that we no longer have a straightforward Weiner–Khinchin connection between spectral and physical-space statistics, as in (12)–(14), or in (15)–(17), is not troublesome. We simply apply (25) to blue-noise media where the high-frequency fluctuations not only lead to an ultraviolet catastrophe but contain increasingly more power as k increases.

This time, the correction term in s^{2H} exceeds in magnitude the presumably dominant term $-\langle\sigma\rangle s$ in $\ln\langle T(s)\rangle$ at very small values of s, specifically, when

$$s<s_0=\frac{(C_\sigma^2/2)^{1/(1-2H)}}{\langle\sigma\rangle}. \tag{29}$$

Here again, we of course never expect $\langle T(s)\rangle$ to exceed unity in reality. This is just another artifact of the ad hoc Gaussian assumption. However, in sharp contrast with the $H>1/2$ case, the fluctuations of τ into negative values become manifest at the smallest values of s. This, in turn, is an interesting consequence of the negative spatial correlations in blue noise that translates to negative correlations noted previously in successive increments of the associated fBm, cf. (18). Undesirable artifacts of the Gaussian variability model can be suppressed in a numerical implementation of the present model, for any value of H, by taking $\tau(x_0,x_1)=\max\{0,\int_{x_0}^{x_1}\mathrm{d}\tau(x)\}$ for every realization of the noises. Otherwise, we require in this regime that

$$(C_\sigma^2/2)^{1/(1-2H)}\ll 1, \tag{30}$$

and also that $s\gg s_0$, thus minimized in (29).

In this previously unexplored regime, the asymptotic (large s) behavior of $\langle T(s)\rangle$ is the standard prediction of Beer's law (approached algebraically from above):

$$\langle T(s)\rangle\sim\exp(-\langle\sigma\rangle s)\times[1+O(s^{-1+2H})]. \tag{31}$$

Shaw et al. [26] predict super-exponential behavior based on a discrete-point process analysis of scenarios where the material particles obstructing the flow of radiation are anti-clustered, i.e., they have negative (repelling) spatial correlations. Our continuum-based approach leads to the same conclusion, although the deviation from exponential decay is weak in the present model.

Now, one can also use the white-noise case in (26) as a benchmark to assess the effects of spatial correlations. In this case, we see that the negatively correlated noises lead for all practical purposes to exponential behavior, but modified from an extinction of $\langle\sigma\rangle[1-C_\sigma^2/2]$ to the *larger* value $\langle\sigma\rangle$. The key Fig. 3 in Shaw et al.'s paper illustrates their numerical simulations of radiation propagation in various realizations of random media generated with a specific rule for enforcing negatively correlated particle positions, at least at short distances. Rather than a clear-cut super-exponential per se, i.e., a qualitatively different decay rate (such as $\mathrm{e}^{-a(\langle\sigma\rangle s)^b}$ with $a>0$ and $b<1$), Shaw et al.'s Fig. 3 shows what seems to be a modified exponential trend in $\langle T(s)\rangle$ with a steeper slope in log-linear axes than predicted by their version of Beer's law, which we identify with the white-noise case.

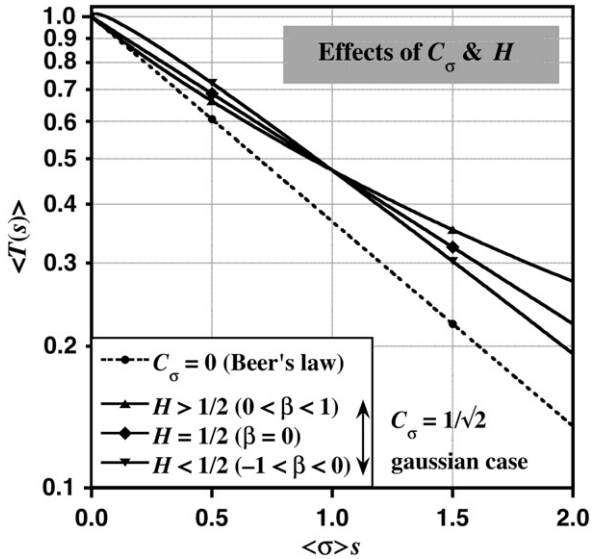

Fig. 3. Mean transmission laws $\langle T(s)\rangle$ for stochastic media modeled with Gaussian white-, pink-, and blue noises from (25) are compared to a uniform media with the same (mean) extinction. Variability amplitude parameter C_σ^2 is either 0 or 1/2; in the latter case, the Hurst exponent H of the associated fBm is set to 1/4 (blue noise), 1/2 (white noise), and 3/4 (pink noise).

At any rate, the present case study establishes that negatively correlated heterogeneous optical media can be handled with conventional RT, albeit at the cost of extending it from regular to merely measurable functions (followed by a restriction to a special, but representative, class of such measures). This contradicts speculation by Kostinski, Shaw, and Lanterman [23,25,26] that only discrete-point process approaches are general enough to accommodate such "super-homogeneous" media where distances between the material's particles are on average larger than predicted by a Poissonian distribution. However, if the two approaches to particle/radiation transport are in fact equivalent, as the evidence presented here seems to show, then both frameworks are enriched by the existence of the alternate one.

5.3. Summary and mitigation of Gaussian artifacts

Fig. 3 summarizes our findings in a log-linear plot of $\langle T(s)\rangle$ versus $\langle\sigma\rangle s$, ranging from 0 to 2. We illustrate cases where $C_\sigma=0$, yielding the standard (uniform medium) model, and where $C_\sigma=1/\sqrt{2}$. In the latter case, the Hurst exponent H of the associated fBm is taken to be 1/4, 1/2, 3/4, but $\langle T(1/\langle\sigma\rangle)\rangle=1/\mathrm{e}^{5/4}\approx 0.47$, irrespective of H. We see that $\langle T(s)\rangle>\mathrm{e}^{-\langle\sigma\rangle s}$ in all cases for all $s>0$. We note the modified exponential behavior predicted in (26) for H = 1/2, and by others (using various arguments) for uncorrelated fluctuations. The sub-exponential trend for H = 3/2 is clearly visible in this case where $\langle\sigma\rangle s^*$ in (27) is $(8/3)^2\approx 7.1$, i.e., appropriately off the chart. Finally, we notice the super-exponential behavior when H = 1/4; specifically, $\ln\langle T(s)\rangle$ is a concave function of s, albeit

rather weakly concave in the physically meaningful regime where $s \gg s_1$ in (29), which is only $1/16 \approx 0.06$ of $1/\langle\sigma\rangle$ (the MFP when $C_\sigma = 0$) in this example.

The Gaussian artifacts, one of which is clearly visible in Fig. 3, can be mitigated if necessary—in particular, for any future application of the model. The constraints here are that we want an analytic expression for the characteristic function for the PDF of $\tau(0,s)$ and, simultaneously, we want to keep a tight handle on its 2-point correlation statistics. One could map, one-to-one, the Gaussian deviates to (near-Gaussian) Gamma-distributed ones with the same 1-point mean $\mu = \langle\sigma\rangle s$ and variance $\nu = (C_\sigma \mu)^{2H}$, but supported by $(0,\infty)$. In lieu of (24), their Laplace-based characteristic function is

$$\langle e^{-\tau\xi}\rangle = \frac{1}{\Gamma(\alpha)}\left(\frac{\alpha}{\mu}\right)^{\alpha}\int_0^\infty \tau^{\alpha-1} e^{-\alpha\tau/\mu}\exp(-\tau\xi)\,d\tau = \frac{1}{(1+\mu\xi/\alpha)^{\alpha}}, \tag{32}$$

where $\alpha = \mu^2/\nu$, which in the present circumstances is assumed $\gg 1$. However, we must also assume that the $(H, C_\sigma; \langle\sigma\rangle s)$−dependent map between $\mathbb{R}$ and $(0,\infty)$, which involves inverse regularized incomplete Gamma functions and error functions, does not change the 2-point correlations. This needs to be verified numerically, an exercise that is outside of our present scope. In the meantime, we revisit in Fig. 4 the cases in Fig. 3 using

$$\langle T(s)\rangle = \langle e^{-\tau}\rangle(s) = \left(1+\frac{\langle\sigma\rangle s}{\alpha(s)}\right)^{-\alpha(s)} \tag{33}$$

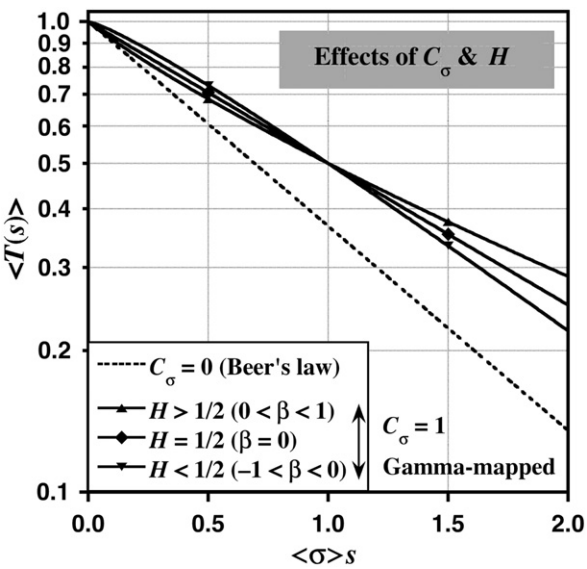

Fig. 4. Same as Fig. 3 but after transforming the Gaussian fBm associated with the scaling noise into a Gamma-distributed one with the same mean and variance, assuming no change in the two-point correlations. $\langle T(s)\rangle$ is obtained from (33) and (34) when H = 1/4,1/2,3/4, and $C_\sigma = 0$ and 1. This log-Gamma model for $T(s)$ does not have the artifacts of the log-normal one in Fig. 3, but its correlation properties are not fully known at present.

from (32) with $\xi = 1$ to retrieve (21). The key variability parameter is now s-dependent:

$$\alpha(s) = \left(\frac{(\langle\sigma\rangle s)^{1-H}}{C_\sigma^H}\right)^2. \tag{34}$$

The magnitude of C_σ is no longer limited in this log-Gamma model and, to obtain sub-exponential behavior of the same magnitude as in Fig. 3, it was increased from $1/\sqrt{2}$ to unity in Fig. 4. In particular, this setting gives us $\langle T(1/\langle\sigma\rangle)\rangle = 1/2$, irrespective of H.

Asymptotically ($s \gg 1/\langle\sigma\rangle$), the transmission law in (33) and (34) reads as a stretched exponential, further enhanced with a logarithmic prefactor, when $H \gtrsim 1/2$:

$$\ln\langle T(s)\rangle = -\frac{(\langle\sigma\rangle s)^{2(1-H)}}{C_\sigma^{2H}} \times \ln[1 + C_\sigma^{2H} \times (\langle\sigma\rangle s)^{2H-1}].$$

The limit $H \to 1^-$ (quasi-continuous extinction fields) leads to an algebraic decay as the $-1/C_\sigma^2$ power of source distance s.[12] Like for the Gaussian model, we find a modified exponential behavior for any value of $\langle\sigma\rangle s$ when H = 1/2. This time, however, the mean extinction is multiplied by $\ln(1+C_\sigma^2)/C_\sigma^2$ (which is less than unity for any value of C_σ). When $H < 1/2$, the expected super-exponential behavior is obtained without the artifact at small s. Indeed the same trend as in (31) is found.

6. Conclusions and potential applications

We surveyed the literature on transport in optical or nuclear-engineering materials with randomly variable macroscopic cross-section from the standpoint of propagation, i.e., the spatial part of the full transport kernel. Using a specific-yet-representative class of Gaussian scaling variability models, we extended the general results obtained by Davis and Marshak [15] in 2004 about systematically sub-exponential transmission laws in heterogeneous optical media with (implicitly, positive) correlations. In that paper, fluctuations were represented by *regular* functions whereas here they are represented by *merely measurable* functions. In other words, we have gone from media where extinction has a well-defined numerical value at almost every point (a countable number of discontinuities can occur) to media where only Lebesgue integrals of the extinction field have well-defined numerical values (there can then be discontinuities everywhere). Simply put, we have gone from stochastically continuous media to very "noisy" media where high spatial frequencies dominate the variability.

Further extension from positively to negatively correlated fluctuating media was also achieved, i.e., we went from decaying (pink) to increasing (blue) power-law wavenumber spectra. We then verified the prediction by Shaw et al. in 2002 [26] that this leads to super-exponential behavior for the mean transmission law, at least in

[12] Interestingly, this is precisely the kind of model for sub-exponential direct transmission assumed in Davis' anomalous transport theory [16]. That model, in turn, was rationalized by Barker et al.'s [61] analysis of high-resolution satellite observations of variable oceanic cloud scenes, finding (to reasonable accuracy) Gamma-distributed cloud optical depths.

comparison with the case of media with flat/white spectra. By the same token, we have established that, contrary to speculation by Kostinski [25], an approach to particle or radiation transport grounded in the continuum framework of the linear Boltzmann equation can indeed accommodate negative correlations (anti-clustering of material particles). However, one must concede that the discrete-point process approach that Kostinski [23] originally introduced into transport theory for positively correlated media (material particle clustering) generalizes more naturally to negative correlations.

We can now state with complete confidence that there is equivalence between the classic continuum-based linear Boltzmann model for radiation transport in heterogeneous media on the one hand, and the interesting new description of transport fundamentals developed by Kostinski and coworkers at Michigan Technological University based on discrete-point process theory on the other hand. The scales most naturally described by point processes are commensurate with the distances between material particles because no one argues that the notion of a position-dependent density then breaks down in view of the Poissonian or non-Poissonian fluctuations of counts in the sample volume. Our noise models cover this regime by never calling for a density, only a finite measure over a finite interval. However, any statement about propagation must cover *optical* distances of $O(1)$, and preferably much more, to be of any physical consequence. This means that, to have *simultaneously* fluctuating particle counts in the sample volume and $O(1)$ optical distance across it, microscopic cross sections must be $\sim$(inter-particle distance)^2. However, the "dilute medium" requirement for RT to be valid is then violated and one must deal with multiple scattering in a wave-theoretic framework; cf. Mishchenko et al.'s review [62] in this Special Issue. It seems that for optically dilute media (each scatterer is in the far-field of each other) discrete-point and continuum-based descriptions should be indistinguishable in their predictions over the full range of optical distances, quasi-transparency to complete opacity. If not RT, particle transport in some ultra-dense astrophysical media (collapsing stellar cores, white dwarfs, neutron stars, etc.) and their terrestrial counterparts (inertial fusion experiments) may satisfy these simultaneous constraints. Their exotic multi-physics may well lead to interesting spatial variability at small scales.

At any rate, this makes us all the more eager to see how Mishchenko's recent derivation of the multiple-scattering vector (polarization-capable) radiative transfer equation from the rigorous principles of statistical electromagnetic wave theory[13] [63, and references therein] can be extended to heterogeneous optical media with extinction fluctuations at all scales and amplitudes of interest. Indeed, Mishchenko's estimate of the impact on Beer's law of essentially sub-mean-free-path clumping is small. This is consistent with our prior prediction [15] and present results for 3D media dominated by high spatial frequency variability, i.e., white and blue noises. It is also consistent with the "atomistic mix" limit (vanishing correlation scale) in stochastic RT theory for Markovian binary media [9]. However, the interesting effects (severe perturbation of Beer's law) occur when the opacity fluctuation scales extend up to and beyond the mean-free-path, which is itself boosted by heterogeneity with respect to the estimate based on the mean extinction [15].

What may be the practical applications of radiation and/or particle transport theory for media with high spatial frequency variability, including negatively correlated fluctuations?

The model used in the present study has three parameters, $\{\langle\sigma\rangle, C_\sigma; H\}$ where $H=(\beta+1)/2$ in the regime of interest ($|\beta|<1$). They need to be determined by direct in situ measurement, or inferred from observable (typically, boundary) fluxes. Details will of course depend on the area of application. However, we suspect that in all cases the 2-point correlation parameter $H(\beta)$ is the most challenging. In climate-driven observational research, it was found that terrestrial boundary-layer clouds such as marine stratocumulus, which matter tremendously in the radiative balance of the Earth's climate, are structured much like admixtures in turbulence ($\sim k^{-\beta}$ wavenumber spectra, with $\beta=5/3$) down to scales of a few meters [33,34, among others]; however, at smaller scales high frequencies have enhanced amplitudes (wavenumber spectrum becomes somewhat shallower than k^{-1}, hence $\beta \lesssim 1$) [35,36]. Although typical mean-free-paths in such clouds are 10s of meters, this small scale structure observed in the liquid water content filed (including intermittent "spikes" indicative of droplet clustering) can leave an imprint on the RT at scales unresolved both by observations and in most current cloud modeling based on computational fluid dynamics. Therefore a mean-field model for propagation such as presented here can be put to good use. We can anticipate the natural occurrence of similar structures in many other turbulent environments where transport processes unfold.

Current remote sensing methods typically assume that $C_\sigma \equiv 0$ in their physics/RT-based retrieval algorithms. At least this is the case for clouds and aerosols; moreover, the medium is assumed to be a uniform plane-parallel slab (thickness L) and the key parameter of interest is (mean, vertical) optical depth $\langle\sigma\rangle L$. In principle, given sufficient observational data (e.g., with multiple viewing directions), one can use the present model to add new unknowns such as C_σ (assuming we can make an educated guess for β). A stochastic RT model applies naturally to unresolved (sub-pixel) variability. If the pixel is large enough to neglect 3D RT adjacency effects, and the variability is slow enough ($\beta>1$) then it has been argued [64] that unresolved variations in cloud optical depth are amenable, like in climate model gridcells [19], to the independent-column approximation. In that scenario, β is irrelevant and only a 1-point variance parameter is required. Since assuming zero variance leads to a biased retrieval of the mean optical

[13] This new microphysical derivation is entirely classical and, as such, dismisses as highly misleading the notion that one can substitute "photon" for, say, "neutron" in the definition of phase-space density underlying the linear transport equation, and thus "derive" the RT equation from kinetic theory. From this strictly radiative transfer perspective, discrete-point process theory is even more at fault since it is all about transported particles interacting with material ones.

depth, setting it to some climatological value should remove at least some of the bias. Next-generation cloud/aerosol retrieval algorithms should account for both unresolved and resolved scene variability in order to improve the accuracy currently achieved.

For this and many other reasons, it is encouraging to see vigorous research efforts into the large-scale effects of small-scale variability, including transport kernels with non-exponential decays. In this Special Issue alone, three articles advance this topic. Bal and Jing [65] present a detailed mathematical analysis of the variances (and covariances) of directly transmitted and singly scattered light at one (or more) boundary points from boundary sources for media with high-frequency variability of amplitude small enough to linearize the exponential transmission law; interestingly, the two broad classes of media they consider, with "short-" and "long-range" correlations, correspond to our cases with $\beta \leq 0$ and $0 < \beta < 1$, respectively. Fichtl and Prinja [66] allow for isotropic scattering as well as absorption in their investigation of azimuthally averaged transport through 1D statistically homogeneous and continuous (hence correlated) random media using the Karhuen–Loève expansion; they too address both means and variances of fluxes everywhere throughout the medium.[14] As previously noted, Larsen and Vasques [30] present a generalized formulation of the integro-differential linear transport equation that allows for non-exponential transmission laws and derive its diffusion limit.

As for the occurrence of negatively correlated ($\beta < 0$) optical media in nature, we mentioned ultra-dense media in Section 5.2, and we redirect the reader for less exotic possibilities, described [26] and critically discussed [15] elsewhere in this Journal. The associated transport kernels with super-exponential behavior may find more relevance to engineering systems, for nuclear applications in particular. As demonstrated by two papers in this Special Issue [67,68], the enhanced safety of pebble-bed reactor designs has motivated a renewed of interest in detailed studies of particle transport in Markovian binary mixtures, which have an essentially flat wavenumber spectrum out to the scale of one or more mean-free-paths. At scales on the order of the pebble radius (~ 3 cm), the centers of closely packed spheres repel each other for obvious mechanical reasons. This close-range negative correlation trend may need to be incorporated into mean-field neutron transport theories to ensure the required level of fidelity, possibly using methods similar to those presented herein. We also find that the small-scale heterogeneity of soft human tissue is a growing concern [69,70] in non-invasive biomedical diagnostics using diffuse optical tomography—a new and interesting outlet for theoretical and computational RT.

[14] These authors adopt, like here (and with the same adverse consequences), Gaussian variability (variance ν_σ) and then move on to more physically realistic log-normal fluctuations. Their preferred choice of correlation structure, however, follows from $G_\sigma(r) = \nu_\sigma \exp(-r/\lambda_c)$ where λ_c is the standard (i.e., "integral") correlation scale. This choice for $G_\sigma(r)$ leads to $E_\sigma(k) = \nu_\sigma \lambda_c/[1+(\lambda_c k)^2]$. Therefore, by our classification, it exhibits $\beta = 0$ (de-correlated, stationary) behavior at large scales and $\beta = 2$ (Bm-like, non-stationary) behavior at small scales, with the latter limit ensuring the required stochastic continuity.

Acknowledgements

This research was supported by the Office of Biological and Environmental Research of the U.S. Department of Energy as part of the Atmospheric Radiation Measurement (ARM) program and Los Alamos National Laboratory's Lab-Directed Research & Development—Exploratory Research (LDRD/ER) program under project 20070483ER. Publication of this paper was supported by the JPL, Caltech, under a Contract with the National Aeronautics and Space Administration. A.D. also thanks Guillaume Bal, Bob Cahalan, Martin Frank, Frank Graziani, Yuri Knyazikhin, Alexander Kostinski, Ed Larsen, Mike Larsen, Shaun Lovejoy, Alexander Marshak, Michael Mishchenko, Jim Morel, Raymond Shaw, and Warren Wiscombe for stimulating discussions about non-exponential transmission laws, non-traditional transport formalism, and the discrete-point process approach to RT.

References

[1] Davis A, Gabriel PM, Lovejoy S, Schertzer D, Austin GL. Discrete angle radiative transfer III: numerical results and meteorological applications. J Geophys Res 1990;95:11,729–42.
[2] Cahalan RF. Bounded cascade clouds: albedo and effective thickness. Nonlinear Proc Geophys 1994;1:156–67.
[3] Cahalan RF, Ridgway W, Wiscombe WJ, Bell TL, Snider JB. The albedo of fractal stratocumulus clouds. J Atmos Sci 1994;51:2434–55.
[4] Cairns B, Lacis AA, Carlson BE. Absorption within inhomogeneous clouds and its parameterization in general circulation models. J Atmos Sci 2000;57:700–14.
[5] Petty GW. Area-average solar radiative transfer in three-dimensionally inhomogeneous clouds: the independently scattering cloudlets model. J Atmos Sci 2002;59:2910–29.
[6] Graziani F. Radiation transport in 3D heterogeneous materials: DNS. In: Proceedings of american nuclear society winter meeting. New Orleans (La), 11/16/2003–11/20/2003, Am Nucl Soc, LaGrange Park (Il), 2003.
[7] Olson GL, Miller DS, Larsen EW, Morel JE. Chord length distributions in binary stochastic media in two and three dimensions. J Quant Spectrosc Radiat Transfer 2006;101:269–83.
[8] Olson GL. Chord length distributions between hard disks and spheres in regular, semi-regular, and quasi-random structures. Ann. Nucl. Energy 2008;35:2150–5.
[9] Pomraning GC. Linear kinetic theory and particle transport in stochastic mixtures. Singapore: World Scientific Publishing; 1991.
[10] Byrne RN. 3D radiative transfer in stochastic media. In: Marshak A, Davis A, editors. 3D radiative transfer in cloudy atmospheres. Heidelberg (Germany): Springer; 2005. p. 385–423 [chapter 7].
[11] Kassianov E, Lane-Veron DE. Stochastic radiative transfer in Markovian mixures: past, present and future. J Quant Spectrosc Radiat Transfer 2011;112:566–76.
[12] Stephens GL. Radiative transfer through arbitrary shaped optical media, part 2—group theory. J Atmos Sci 1988;45:1836–48.
[13] Stephens GL. Radiative transfer through arbitrary shaped optical media, part 1—a general method of solution. J Atmos Sci 1988;45:1818–36.
[14] Davis A, Marshak A. Lévy kinetics in slab geometry: scaling of transmission probability. In: Novak MM, Dewey TG, editors. Fractal frontiers. Singapore: World Scientific; 1997. p. 63–72.
[15] Davis AB, Marshak A. Photon propagation in heterogeneous optical media with spatial correlations: enhanced mean-free-paths and wider-than-exponential free-path distributions. J Quant Spectrosc Radiat Transfer 2004;84:3–34.
[16] Davis AB. Effective propagation kernels in structured media with broad spatial correlations, illustration with large-scale transport of solar photons through cloudy atmospheres. In: Graziani F, editor. Computational methods in transport—Granlibakken 2004, Lecture notes in computational science and engineering, vol. 48. New York (NY): Springer; 2006. p. 84–140.
[17] Mullamaa Ü-AR, Sulev MA, Põldmaa VK, Ohvril HA, Niilisk HJ, Allenov MI, Chubakov LG, Kuusk AE. Stochastic structure of cloud and radiation fields. In: Mullamaa Ü-AR, editor. IPA, Acad Sci Est SSR, Tartu, 282pp (in Russian: 1972, English translation: 1975), Technical Report TT F-822, NASA Technical Translation, Washington (DC); 1975.

[18] Cahalan RF, Ridgway W, Wiscombe WJ, Gollmer S, Harshvardhan. Independent pixel and monte carlo estimates of stratocumulus albedo. J Atmos Sci 1994;51:3776–90.
[19] Barker HW. A parameterization for computing grid-averaged solar fluxes for inhomogeneous marine boundary layer clouds—part 1, methodology and homogeneous biases. J Atmos Sci 1996;53:2289–303.
[20] Pincus R, Barker HW, Morcrette JJ. A fast, flexible, approximate technique for computing radiative transfer in inhomogeneous cloud fields. J Geophys Res D 2003;108:4376–9.
[21] Räisäsen P, Barker HW. Evaluation and optimization of sampling errors for the Monte Carlo independent column approximation. Q J R Meteorol Soc 2004;130:2069–85.
[22] Barker HW, Cole JN, Morcrette J, Pincus R, Räisänen P, von Salzen K, Vaillancourt PA. The monte carlo independent column approximation: an assessment using several global atmospheric models. Q J R Meteorol Soc 2008. doi:10.1002/qj.303.
[23] Kostinski AB. On the extinction of radiation by a homogeneous but spatially correlated random medium. J Opt Soc Am A 2001;18:1929–33.
[24] Borovoi AG. On the extinction of radiation by a homogeneous but spatially correlated random medium: comment. J Opt Soc Am A 2002;19:2517–20.
[25] Kostinski AB. On the extinction of radiation by a homogeneous but spatially correlated random medium: reply to comment. J Opt Soc Am A 2002;19:2521–5.
[26] Shaw RA, Kostinski AB, Lanterman DD. Super-exponential extinction of radiation in a negatively-correlated random medium. J Quant Spectrosc Radiat Transfer 2002;75:13–20.
[27] Buldyrev SV, Gitterman M, Havlin S, Kazakov AYa, da Luz MGE, Raposo EP, Stanley HE, Viswanathan GM. Properties of Lévy flights on an interval with absorbing boundaries. Physica A 2001;302:148–61.
[28] Scholl T, Pfeilsticker K, Davis AB, Baltink HK, Crewell S, Löhnert U, Simmer C, Meywerk J, Quante M. Path length distributions for solar photons under cloudy skies: comparison of measured first and second moments with predictions from classical and anomalous diffusion theories. J Geophys Res 2006;D111:12,211–26.
[29] Larsen EW. A generalized Boltzmann equation for "non-classical" particle transport. In: Proceedings of joint international topical meetings on mathematics and computations and supercomputing in nuclear applications (M&C+SNA 2007). Monterey (CA), April 15–19, 2007, Am Nucl Soc, LaGrange Park (Il); 2007, available on CD-ROM.
[30] Larsen EW, Vasques R. A generalized Boltzmann equation for non-classical particle transport. J Quant Spectrosc Radiat Transfer 2011;112:619–31.
[31] Vasques R, Larsen EW. Anisotropic neutron diffusion in model 2-d pebble bed reactor cores. In: Proceedings of conference on mathematics and computations and reactor physics (M&C2009). Saratoga Springs (NY), May 3–7, 2009, Am Nucl Soc, LaGrange Park (Il); 2009, available on CD-ROM.
[32] van Kampen NG. Stochastic processes in physics and chemistry. Amsterdam (The Netherlands): North-Holland/Elsevier; 1992.
[33] Davis A, Marshak A, Wiscombe WJ, Cahalan RF. Multifractal characterizations of non-stationarity and intermittency in geophysical fields: observed, retrieved, or simulated. J Geophys Res 1994;D99:8055–72.
[34] Davis A, Marshak A, Wiscombe WJ, Cahalan RF. Scale-invariance in liquid water distributions in marine stratocumulus, part I, spectral properties and stationarity issues. J Atmos Sci 1996;53:1538–58.
[35] Davis AB, Marshak A, Gerber H, Wiscombe WJ. Horizontal structure of marine boundary-layer clouds from cm- to km-scales. J Geophys Res 1999;D104:6123–44.
[36] Gerber H, Boers R, Jensen J, Davis A, Marshak A, Wiscombe WJ. Spectral density of cloud liquid water content at high frequencies. J Atmos Sci 2001;58:497–503.
[37] Marshak A, Knyazikhin Y, Larsen ML, Wiscombe WJ. Small-scale drop size variability: empirical models for drop-size-dependent clustering in clouds. J Atmos Sci 2005;62:551–8.
[38] Jensen JLWV. Sur les fonctions convexes et les inégalitiés entre les valeurs moyennes. Acta Math 1906;30:175–93.
[39] Schwartz L. Théorie des distributions. Paris (France): Hermann; 1950.
[40] Frisch U. From global scaling, à la Kolmogorov, to local multifractal scaling in fully developed turbulence. Proc R Soc London A 1991;434: 89–99.
[41] Davis A, Lovejoy S, Schertzer D. Radiative transfer in multifractal clouds. In: Lovejoy S, Schertzer D, editors. Scaling, fractals and nonlinear variability in geophysics. Hingham (MA): Kluwer; 1991. p. 303–18.
[42] Mandelbrot BB. Fractals: form, chance, and dimension. San Francisco (CA): W.H. Freeman; 1977.
[43] Knyazikhin Y, Kranigk J, Myneni RB, Panfyorov O, Gravenhorst G. Influence of small-scale structure on radiative transfer and photosynthesis in vegetation canopies. J Geophys Res D 1998;103:6133–44.
[44] Knyazikhin Y, Marshak A, Wiscombe WJ, Martonchik J, Myneni RB. A missing solution to the transport equation and its effect on estimation of cloud absorptive properties. J Atmos Sci 2002;59:3572–85.
[45] Watson BP, Lovejoy S, Grosdidier Y, Schertzer D. Scattering in thick multifractal clouds, part I: overview and single scattering. Phys A Stat Mech Appl 2009;388:3695–710.
[46] Gabriel PM, Lovejoy S, Davis A, Schertzer D, Austin GL. Discrete angle radiative transfer II: renormalization approach for homogeneous and fractal clouds. J Geophys Res 1990;95:11,717–28.
[47] Lovejoy S, Gabriel PM, Davis A, Schertzer D, Austin GL. Discrete angle radiative transfer I: scaling, similarity, universality and diffusion. J Geophys Res 1990;95:11,699–715.
[48] Davis A, Lovejoy S, Schertzer D. Discrete angle radiative transfer in a multifractal medium. In: Varadan VK, editor. Wave propagation and scattering in varied media II, S.P.I.E. proceedings, vol. 1558. Bellingham (WA): S.P.I.E. Publications; 1991. p. 37–59.
[49] Lovejoy S, Watson BP, Grosdidier Y, Schertzer D. Scattering in thick multifractal clouds, part II: multiple scattering. Phys A Stat Mech Appl 2009;388:3711–27.
[50] Lovejoy S. The area-perimeter relation for rain and clouds. Science 1982;216:185–7.
[51] Siebesma AP, Jonker HJJ. Anomalous scaling of cumulus cloud boundaries. Phys Rev Lett 2000;85:214–7.
[52] Knyazikhin Y, Marshak A, Larsen MI, Wiscombe WJ, Martonchik J, Myneni RB. Small-scale drop size variability: impact on estimation of cloud optical properties. J Atmos Sci 2005;62:2555–67.
[53] Bartle RG. The elements of integration and lebesgue measure. New York (NY): John Wiley & Sons; 1995.
[54] Monin AS, Yaglom AM. Statistical fluid mechanics. Boston (MA): MIT Press; 1975 vol. 2.
[55] Papoulis A, Pillai SU. Probability, random variables and stochastic processes. New York, NY: McGraw-Hill Science/Engineering/Mathematics; 2001.
[56] Lampard DG. Generalization of the wiener–Khintchine theorem to nonstationary processes. J Appl Phys 1954;25:802–3.
[57] Mallat S. A wavelet tour of signal processing. San Diego (CA): Academic Press; 1999.
[58] Liou KN. An introduction to atmospheric radiation. 2nd ed.. San Diego (CA): Academic Press; 2002.
[59] Stephens GL, Gabriel PM, Tsay S-C. Statistical radiative transport in one-dimensional media and its application to the terrestrial atmosphere. Transp Theory Stat Phys 1991;20:139–75.
[60] Newman WI, Lew JK, Siscoe GL, Fovell RG. Systematic effects of randomness in radiative transfer. J Atmos Sci 1995;52:427–35.
[61] Barker HW, Wielicki BA, Parker L. A parameterization for computing grid-averaged solar fluxes for inhomogeneous marine boundary layer clouds—part 2, validation using satellite data. J Atmos Sci 1996;53:2304–16.
[62] Mishchenko MI, Tishkovets VP, Travis LD, Dlugach JM, Liu L, Rosenbush VK, Kiselev NN. Electromagnetic scattering by a morphologically complex object: fundamental concepts and common misconceptions. J Quant Spectrosc Radiat Transfer 2011;112: 671–92.
[63] Mishchenko MI. Multiple scattering, radiative transfer, and weak localization in discrete random media: unified microphysical approach. Rev Geophys 2008;46:RG2003, doi: 10.1029/2007RG000230.
[64] Kokhanovsky AA. The influence of the horizontal inhomogeneity on radiative characteristics of clouds: an asymptotic case study. IEEE Trans Geosci Remote Sens 2003;41:817–25.
[65] Bal G, Jing W. Fluctuation theory for radiative transfer in random media. J Quant Spectrosc Radiat Transfer 2011;112:660–70.
[66] Fichtl ED, Prinja AK. The stochastic collocation method for radiation transport in random media. J Quant Spectrosc Radiat Transfer 2011;112:646–59.
[67] Brantley PS. A benchmark comparison of Monte Carlo particle transport algorithms for binary stochastic mixtures. J Quant Spectrosc Radiat Transfer 2011;112:599–618.
[68] Griesheimer DP, Millman DL, Willis CR. Analysis of distances between inclusions in finite binary stochastic materials. J Quant Spectrosc Radiat Transfer 2011;112:577–98.
[69] Shah N, Cerussi AE, Jakubowski D, Hsiang D, Butler J, Tromberg BJ. Spatial variations in optical and physiological properties of healthy breast tissue. J Biomed Opt 2004;9:534–40, doi: 10.1117/1.1695560.
[70] Svensson T, Swartling J, Taroni P, Torricelli A, Lindblom P, Ingvar C, Andersson-Engels S. Characterization of normal breast tissue heterogeneity using time-resolved near-infrared spectroscopy. Phys Med Biol 2005;50:2559–71.